Estimation of surface noise source level from low-frequency seismoacoustic ambient noise measurements

Henrik Schmidt
Massachusetts Institute of Technology, Cambridge, Massachusetts 02139

W. A. Kuperman
Naval Research Laboratory, Washington, DC 20375

(Received 12 April 1988; accepted for publication 10 August 1988)

The waveguide nature of a shallow water environment bounded below by a viscoelastic medium permits noise to couple into seismic waves. Geophone and hydrophone measurements have shown that below a threshold frequency of about 10 Hz in 100 m of water, there is a large increase in the measured noise levels, with a peak at approximately 0.25 Hz. A previously developed wave theory of distributed noise in a waveguide has been combined with a full wave solution technique for stratified elastic media and used for numerical modeling and analysis of this phenomenon. It is demonstrated that this low-frequency increase in noise level is only partly due to an increase in the source spectral level. At these frequencies, seismic interface waves become important propagation paths for the ambient noise, leading to a significant magnification of the observed noise levels. This strongly suggests that propagation effects have to be accounted for when evaluating source theories by comparison to experimental data.

PACS numbers: 43.30.Nb, 43.30.Bp

INTRODUCTION

The spatial structure of low-frequency noise from distributed sources such as those causing surface-generated noise in deep or shallow water is governed by the waveguide defined by the water column bounded above by a pressure release surface and below by a stratified viscoelastic medium. Therefore, in determining the actual source spectrum level of the noise-generating sources from measured data, it is necessary to account for or "subtract out" the ocean waveguide environment. Only after this procedure is followed can source levels be derived from noise measurements performed in arbitrary ocean environments and, consequently, be compared between experiments performed in different environments and seasons.

In this article we apply a wave theory of surface-distributed noise in a stratified ocean to data collected in a low-frequency shallow water experiment. The results explain the waterborne and seismic partitioning of low-frequency distributed noise in shallow water. This same analysis applies to the wavelength-scaled deep water distribution of surface-generated noise. By accounting for the ocean environment in a set of diverse experiments previously summarized by Kibblewhite and Ewans,[1] we find that the spread of the reported noise source levels as a function of frequency and parametrized by the wind/sea state is considerably reduced over the levels originally reported, which took the noise measurements as the noise source levels. Not only does this demonstrate the importance of including propagation factors in processing noise data for estimating source levels, but the results indicate a consistency in the frequency dependence of the noise source levels, which suggests that there is only one (or possibly two) dominant natural noise source mechanism that contributes to ambient noise below 10 Hz.

At intermediate frequencies and above, the acoustic waveguide nature of the noise field has been reported previously.[2–4] Recently, Ingenito and Wolf[5] have studied the site dependence of shallow water noise data in terms of waveguide theory.[2] At lower frequencies, the stratified ocean environment supports not only body waves, but also surface waves associated with the interfaces of the layers. Whether or not discrete modes exist in the environment, there exist interface waves in a viscoelastic environment which are never cut off.[6] The amplitude distribution of a surface wave decays exponentially away from the guiding interface, which implies that interface waves can only be excited by sources close (in terms of wavelength) to the interface, a condition normally satisfied for ocean bottom interfaces at acoustic frequencies below cutoff. Hence, at frequencies below waterborne propagation cutoff, these interface waves provide a mechanism for sound, including ambient noise, to be propagated and sensed in the water column and on the seabed in particular. This partitioning between body and interface waves provides an explanation for the spectral distribution of noise observed experimentally in shallow water[1,7] and also reported elsewhere for deep water environments,[8–10] where it is believed that some sort of activity at the air/sea interface is the source of low-frequency noise often referred to as microseisms.[11]

In Sec. I of this article the theory that describes the distribution of surface-generated noise is summarized and modified to include expressions for the vector quantities that a seismic sensor with three geophones would measure. It is shown that this theory predicts with decreasing frequency below cutoff a large increase in the vertical and radial components of the outputs of the geophone as compared to a much smaller increase from the pressure output of an adjacent hydrophone. Above cutoff, the noise spectrum level oscillates in amplitude as a function of frequency, corresponding to the cutoffs of the individual modes, as seen experimentally, for example, in deep water data.[12]

We next describe a shallow water experiment with an ocean bottom seismometer (OBS) and present its results, which are consistent with the theoretical predictions. Since the theory predicts only relative levels because the spectral level of the noise sources is an unknown input, the experiment combined with theory can be used to derive the spectral distribution of the noise sources. Then, the same procedure is applied to other shallow water data as summarized in Ref. 1, and, finally, the water depth dependence of the spectral distribution is investigated.

It is demonstrated that the excitation of seismic waves below waterborne mode cutoff accounts for a significant frequency-dependent "magnification" in observed noise levels as compared to the actual source levels. Accounting for the propagation in the spectral distribution of noise is therefore crucial at low frequencies, resulting in a significantly lower spread in the derived source levels as opposed to the spread of the directly measured noise levels. Further, this procedure will separate propagation from sea state effects.

It should be stressed that the present article is not intended as a contribution to the ongoing discussion concerning the nature of the source mechanisms,[13] but rather as a theoretically derived statement based on existing data of the importance of properly accounting for propagation effects when evaluating different theories by comparison to experimental data.

I. THEORY

In this section we summarize and extend the results of a previous article[2] to include the description of the velocity components of the seismic field expected to be measured by geophones.

The theory is based on the environmental geometry model shown in Fig. 1. The environment is assumed to be horizontally stratified, with a water column with sound-speed profile $c(z)$ overlying a stratified, elastic bottom with the compressional velocity c_P and shear velocity c_S constant within each layer. The sources of the surface-generated noise

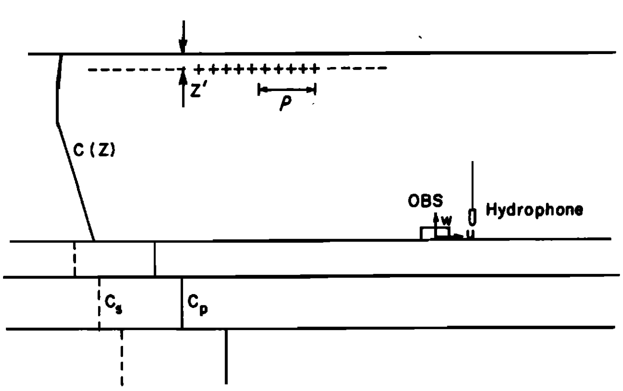

FIG. 1. Modeling of surface-generated ambient noise in a range-independent ocean environment. The sources are assumed to be a horizontally uniform distribution of acoustic monopoles at depth z', with a horizontal correlation $N(\rho)$. The ocean environment is described by a water column of thickness H, with the sound-speed profile $c(z)$. The bottom is assumed to be a horizontally stratified elastic half-space.

are simulated by a distribution of monopole sources at depth z'. The source distribution is assumed to be horizontally homogeneous and isotropic with correlation $N(\rho)$, where ρ is the horizontal distance between two sources.

In such a stratified medium an exact integral representation for the seismoacoustic field is obtained by separation of variables. In a Cartesian coordinate system, Fourier transformation of the wave equation leads to the following expression for the acoustic velocity (or displacement) potential at the angular frequency ω:

$$G(\mathbf{r},\mathbf{r}';z,z') = \frac{1}{2\pi} \int d^2\mathbf{k}\, g(k;z,z') \exp[i\mathbf{k}(\mathbf{r}-\mathbf{r}')] , \tag{1}$$

where the primes denote the source coordinates. The integral in Eq. (1) is performed over all horizontal wave vectors $\mathbf{k}$, and the kernel $g(k;z,z')$ is the depth-dependent Green's function satisfying the differential equation

$$\frac{d^2g}{dz^2} + [K^2(z) - k^2]g = -\frac{1}{2\pi}\delta(z-z') , \tag{2}$$

where $K(z) = \omega/c(z)$. In the case of elastic media the field can be expressed in terms of three displacement potentials: one for compressional waves (P), one for vertically polarized shear waves (SV), and one for horizontally polarized shear waves (SH).[14] The SH waves are not excited by the compressional monopole sources treated here and the associated potential can therefore be discarded. The P and SV potentials both have integral representations of the form given in Eq. (1), with the kernels satisfying depth-separated wave equations similar to Eq. (2). The method applied here for solving the depth-separated wave equations is the global matrix approach described in detail in Refs. 15 and 16 and implemented in the SAFARI code.[17]

Once solved for the depth-dependent Green's functions, the expectation value of acoustic pressure intensity due to a distribution of monopole sources is obtained as[2]

$$\langle |p^2(z)| \rangle = 2\pi\omega^2 q^2 \int d^2\mathbf{k}\, P(\mathbf{k}) |g(k;z,z')|^2 , \tag{3}$$

where q is the spectral source level for the acoustic monopoles generating the noise [see Eqs. (10) and (11) of Ref. 2] and $P(\mathbf{k})$ is the spatial wave vector spectrum of the distributed noise sources, i.e., the Fourier transform of the correlation function. As shown by Kuperman and Ingenito,[2] the correlation function of surface sources, which produce a far-field radiation (of multipole order m) pattern $\cos^m \theta$ with respect to vertical, is given by

$$N(\rho) = \begin{cases} 2\delta(K(z')\rho)/[K^2(z')\rho], & m=1, \\ 2^m m! \{J_m[K(z')\rho]/[K(z')\rho]^m\}, & m>1. \end{cases} \tag{4}$$

The components of the particle velocity are obtained by differentiating the wave field potentials with respect to the spatial coordinates,[16] leading to expressions similar to Eq. (3) for these components.

Since the environment, as well as the source distribution, is horizontally isotropic, the integration is conveniently carried out in cylindrical geometry. Then, for all m of Eq. (4), we obtain from Eq. (3) after some mathematical manipulation and integration over the azimuthal coordinate[2,3] the expectation I of the square of the pressure and velocity components:

$$I=\frac{8\pi m q^2}{K^{2m}(z')}\int_0^\infty |g_{p,w,u}(k;z,z')|^2[K^2(z')-k^2]^{m-1}k\,dk\,, \tag{5}$$

where g_p is the depth-dependent Green's function for the pressure and g_w and g_u are those for the vertical and horizontal components of the particle velocity, respectively.

In order to eliminate the dependence on the unknown source depth z', the monopole source strength q is normalized to yield the pressure level Q in an infinitely deep ocean, independent of the actual value of z'. This is accomplished to first order in z' if q^2 is assigned the value

$$q^2(z')=Q^2/16\pi(z')^2\,. \tag{6}$$

Provided z' is chosen small compared to the vertical wavelengths involved in the integral, evaluation of Eq. (5) will be approximately independent of z'.

When stating source strengths in the following, we will therefore not refer to the depth-dependent value of q, but rather to the value of Q, corresponding to the pressure produced by the same source distribution in an infinitely deep ocean. For example, when we state a noise source level of 50 dB, this value corresponds to Q, resulting in a uniform 50-dB pressure level in a homogeneous semi-infinite half-space. This particular normalization is identical to the one used in Refs. 3 and 4 for $m=1$. For $m>1$, however, there is a factor m difference in the expression for the monopole strength, Eq. (6). For the same "source level," Ref. 3 therefore obtains different pressure levels in a half-space for different values of m, in contrast to the present formulation.

Plotting of the depth-dependent Green's functions, i.e., the kernels $g(k;z,z')$ of Eq. (5) as a function of horizontal wavenumber k, is very instructive and useful for the analysis of the important propagation mechanisms in different frequency regimes. To illustrate this, we choose the scenario of the experiment to be discussed in Sec. II. A simplified model for the actual environmental parameters is given in Fig. 2. Characteristic values for silt and coarse sand were used for the 10-m-thick sediment layer and the subbottom, respectively.[18] The Green's functions are plotted in Fig. 3 for 10, 5, and 1 Hz. The narrow, *discrete* (modal) spectrum interval is indicated in the figures; the region to the left is the *continuous* portion of the spectrum corresponding to more vertical propagation ($k=0$ corresponds to vertical propagation) and bottom interface waves will appear to the right of the discrete spectrum since these *evanescent* waves have phase speeds slower than the speed of sound in the water column (large k). At 10 Hz, we see that the Green's functions for all three motions have a peak in the discrete region corresponding to the normal mode propagation regime. At 5 Hz all normal modes have been cut off, and the Green's functions are dominated by the *continuous* part of the spectrum. At this frequency, peaks appear to the right of the discrete region, corresponding to the existence of interface waves.[6] Finally, at 1 Hz, Fig. 3(c), the Green's functions are dominated by high amplitude peaks corresponding to the fundamental interface (or Scholte) mode.

It is important to note the difference in interpreting the

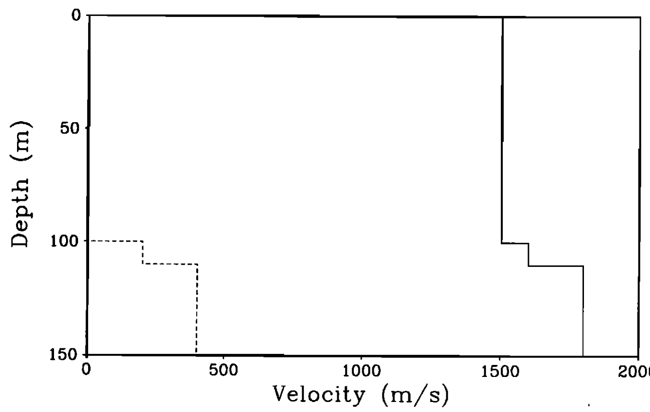

FIG. 2. Environmental model used for modeling surface-generated ambient noise on the Ligurian shelf. The water depth is 100 m, and the sound speed is assumed to be constant, 1500 m/s. The bottom is represented by a silt layer of thickness 10 m overlying a homogeneous sand half-space, with the compressional and shear speeds indicated by the solid and dashed lines, respectively. The density of the silt layer is 1.8 g/cm^3 and the attenuations are 0.5 dB/λ for compressional waves and 1.0 dB/λ for shear waves. The corresponding values for the subbottom are 2.0 g/cm^3, 0.1 dB/λ, and 0.2 dB/λ. The acoustic pressure and particle velocities are simulated as recorded by a hydrophone and a three-component geophone station on the seabed.

Green's functions of Fig. 3 in the case of signal propagation from discrete sources and in the present case of propagation from horizontally distributed sources. In the case of a discrete signal, the complex values of $g(k;z,z')$ are multiplied by an oscillating exponential function $\exp(-ikr)$[15] or a Bessel function $J_m(kr)$.[16] As a result of cancellation, this has the effect that, for long ranges r, a wide peak in the kernel will contribute less than a narrow peak, or in other words, the width of a peak is a measure of the range attenuation of the corresponding mode. As is well known, the Scholte mode of Fig. 3(c), although highly excited, will attenuate rapidly in range.[19,20] The same is the case for the *continuous* spectrum. On the other hand, the sharpness of the modal peak in Fig. 3(a) indicates that this mode will propagate over long distances.

In the present case, however, the integration over the horizontal source plane eliminates the oscillating exponential or Bessel functions. Thus, as seen in Eq. (5), the wavenumber integration is performed directly on the kernel amplitudes (except for the smooth wavenumber factor). A wide peak will therefore contribute not only according to its peak level, but also as a result of its width. The noise field obtained by integrating the Green's functions in Fig. 3(c) will therefore be dominated by the highly excited and wide peak corresponding to the Scholte mode. In contrast, the highly excited normal mode in Fig. 3(a) will not alone dominate the noise field since the *continuous* spectrum is significantly wider. As also demonstrated by Hamson,[3] the contributions from the *discrete* and *continuous* spectra are therefore comparable in significance in the modal propagation regime.

Since the width of the peaks in Fig. 3 is a measure of the propagation attenuation of the corresponding modes, it can be concluded from Fig. 3(b) and (c) that below the cutoff

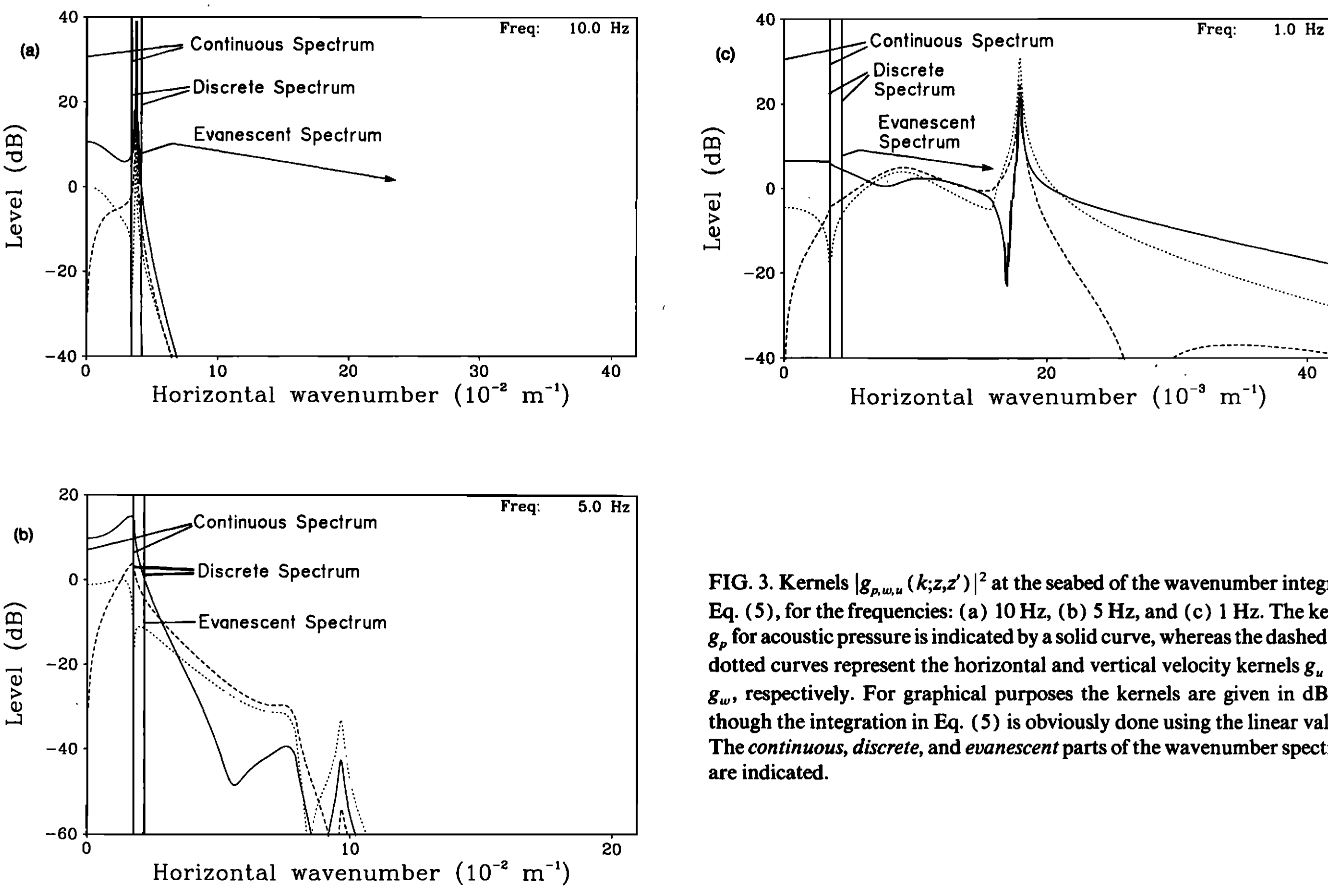

FIG. 3. Kernels $|g_{p,w,u}(k;z,z')|^2$ at the seabed of the wavenumber integrals, Eq. (5), for the frequencies: (a) 10 Hz, (b) 5 Hz, and (c) 1 Hz. The kernel g_p for acoustic pressure is indicated by a solid curve, whereas the dashed and dotted curves represent the horizontal and vertical velocity kernels g_u and g_w, respectively. For graphical purposes the kernels are given in dB, although the integration in Eq. (5) is obviously done using the linear values. The *continuous*, *discrete*, and *evanescent* parts of the wavenumber spectrum are indicated.

frequency for the normal modes, the noise field will be dominated by sources at relatively short ranges: in the present case a few kilometers. This, in turn, justifies the use of a range-independent propagation model for predicting the ambient noise levels in this frequeny regime, a statement supported by the excellent aggreement with experimental data presented in the following.

Figure 4 schematically summarizes the significance of the different spectral regimes for the Green's functions. For 10 Hz, *discrete* modal propagation at shallow grazing angles contributes significantly to the structure of the noise. As the wavelength increases, the discrete modes are cut off [5 Hz, Fig. 3(b)], leaving mainly contributions from the steeply propagating *continuous* spectrum. Figure 4 also indicates the depth dependence of the evanescent Scholte wave at two different frequencies, illustrating how an increase in wavelength moves the surface noise sources into the nearfield of the interface wave (or vice versa) and explaining the dominant excitation of the seismic interface waves in Fig. 3(c).

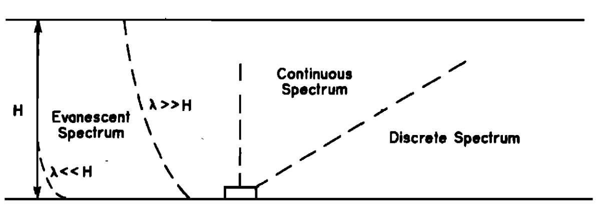

FIG. 4. Schematic representation of the three spectral regimes. The *continuous* spectrum corresponds to plane waves propagating at grazing angles larger than critical, thus undergoing significant bottom loss. The *discrete* part of the spectrum contains the normal modes, which, as a result of their low bottom loss, contribute significantly to the detected noise field above cutoff, as illustrated in Fig. 3(a). In the *evanescent* regime the wave field consists of inhomogeneous plane waves traveling horizontally, with amplitudes exponentially decaying away from the seabed. This spectral regime contains the seismic interface waves, which become the most important propagation mechanism below the modal cutoff frequency, as illustrated in Fig. 3(c).

Figure 5 shows the result of evaluating the wavenumber integrals of Eq. (5) for $m = 1$ and frequencies in the 0- to 100-Hz range, assuming a "white" source spectrum level of $Q = 70$ dB. Figure 5(a) indicates the predicted hydrophone pressure (solid curve), horizontal geophone level (dashed curve), and vertical geophone level (dotted curve). The spectral dB levels for the pressure are relative to 1 μPa/$\sqrt{\text{Hz}}$, whereas the levels for the particle velocities are relative to 10^{-6} μm/s/$\sqrt{\text{Hz}}$. Figure 5(b) indicates the corresponding results for a fluid bottom not supporting shear.

In Fig. 5(a), a rapid rise in the noise level appears at the cutoff frequency of 8 Hz for the first normal mode. The local maximum at approximately 10 Hz corresponds to the optimal combination of the excitation and attenuation of the first mode. Similarly, the "local" increases in the spectral level at higher frequencies are associated with the cutoff process for the higher-order modes. At lower frequencies, the predicted noise levels decrease because there are no discrete contributions from distant noise sources, leaving mainly the contributions from the *continuous* spectrum [Fig. 3(b)]. Finally,

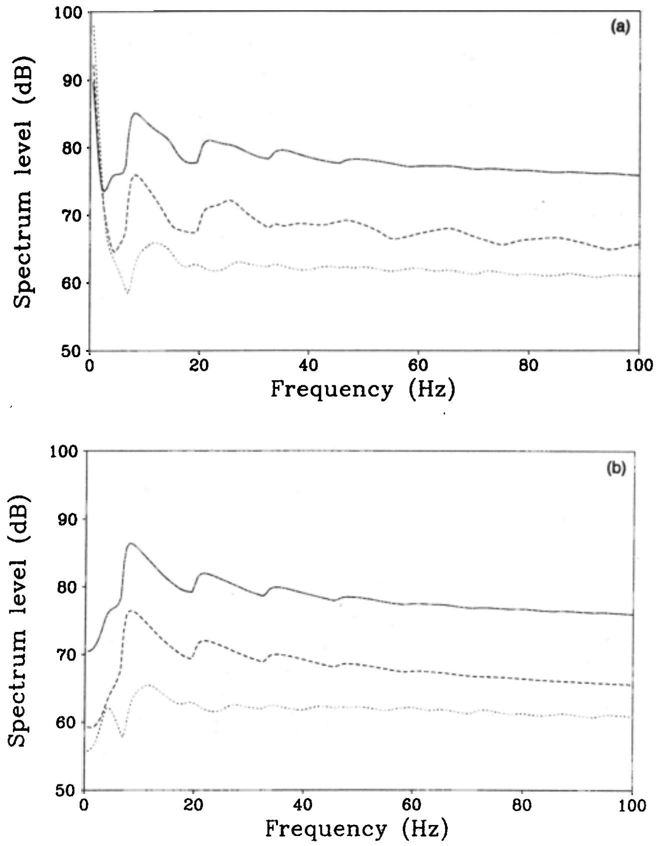

FIG. 5. Simulated frequency spectrum of ambient noise below 100 Hz, obtained by evaluating the wavenumber integrals in Eq. (5) with $m = 1$ and a value of q^2 that in an infinitely deep ocean would yield a uniform pressure amplitude of Q^2 corresponding to 70 dB. The pressure spectrum is indicated by a solid line, whereas the dashed and dotted lines correspond to the horizontal and vertical particle velocities, respectively. Figure 5(a) shows the result for an elastic bottom, whereas Fig. 5(b) shows the result if bottom shear properties are ignored. The effect of correctly treating the elastic bottom is particularly evident below the modal cutoff frequency of 8 Hz.

at very low frequencies, there is a significant increase in the noise due to the fact that the surface noise sources are in the nearfield of the bottom and highly excite interface waves, as demonstrated in Fig. 3(c). As a result of the surface pressure release effect, the increase is greater for the particle motion detected by geophones than for the hydrophone pressure. This low-frequency excitation would not occur for a purely fluid bottom that cannot support seismic interface waves, as illustrated in Fig. 5(b).

II. EXPERIMENT

A recent experiment by Akal *et al.*[7] motivated this study of seismoacoustic noise in the context of the waveguide interpretation of the spectral partitioning of noise.

A. Description of experiment and results

The setup for the experiment is illustrated in Fig. 6. The ambient noise was recorded by means of a three-component geophone station (OBS) and a hydrophone close to the seabed in a relatively flat area of the Italian Ligurian shelf with 100-m water depth. The sea state was measured with a

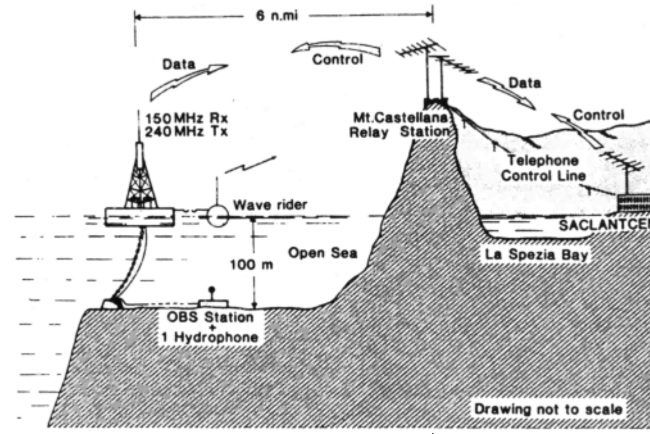

FIG. 6. Experimental setup used by Akal *et al.*[7] for recording ambient noise on the Ligurian shelf. At a position with a water depth of 100 m, an OBS and a hydrophone were placed on and just above the seabed, respectively. The seismoacoustic data were transmitted to a shore station via a radio link, together with surface wave data recorded by a wave rider buoy.

wave rider and the data were continuously transferred to a shore station via radio link. Data were recorded during a period of 105 days, with acquisition in daily 5-min periods.

Figure 7 shows a characteristic example of the noise spectrum obtained during a period having a prevalent sea state 2 (30- to 60-cm significant waveheight) with little shipping. The solid line indicates the power spectrum in dB/(1 μPa)^2/Hz for the hydrophone, whereas the dashed and dotted curves represent the power spectra for a horizontal and vertical geophone, respectively, given in dB/($10^{-6}\,\mu$m/s)^2/Hz. Only one horizontal component is shown, but it was a general feature in periods of no nearby shipping that the two horizontal components registered almost identical spectra, indicating an isotropic noise field under these conditions.

B. Comparison with theory for the extraction of noise source levels

From the theory discussed in Sec. I, it is clear that we can extract the noise source level from the experimental data

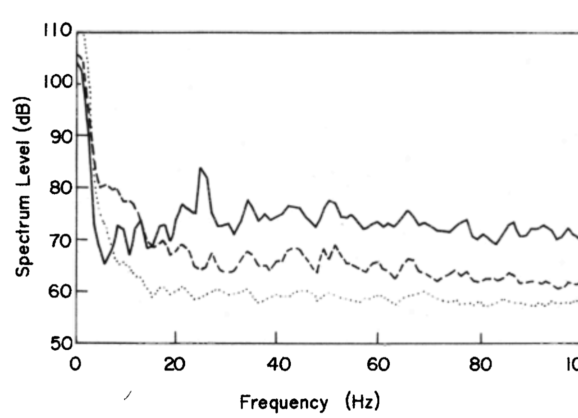

FIG. 7. Characteristic example of noise data recorded under sea state 2 conditions in a period with low nearby shipping density. The frequency spectrum for the hydrophone data is indicated by a solid curve, whereas the horizontal and vertical particle velocity spectra are represented by the dashed and dotted curves, respectively.

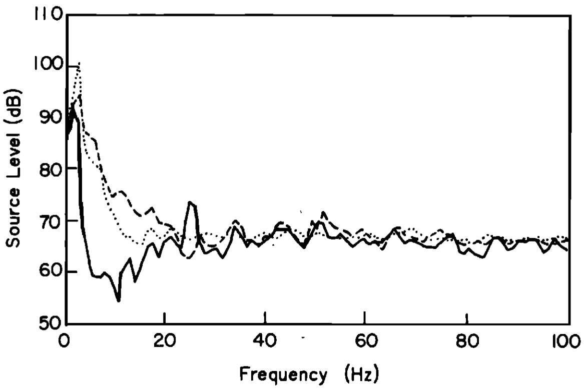

FIG. 8. Source levels for surface generated ambient noise on the Ligurian shelf at sea state 2 obtained by subtracting the model predictions of Fig. 5(a) from the experimental data shown in Fig. 7. The solid curve indicates the source spectrum so obtained from the hydrophone data, whereas the dashed and dotted curves shows the spectra obtained from the two geophone components. At frequencies below 20 Hz, the source levels obtained from the hydrophone data drop off as a result of the low-frequency cutoff of the hydrophones.

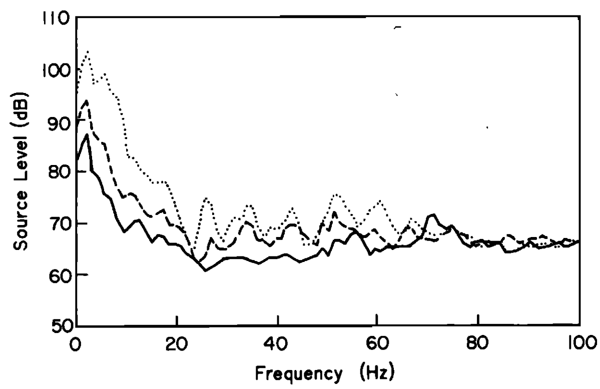

FIG. 9. Source levels on the Ligurian shelf derived from horizontal geophone data at sea states 0 (solid curve), 2 (dashed curve), and 6 (dotted curve).

represented in Fig. 7 by simply taking the difference (in dB's) between Eq. (5) and the data for each frequency. Figure 8 is the noise source level as obtained by this procedure using sea state 2 data. That we obtain the same noise source level from the geophones and hydrophone (with the exception of the hydrophone's low-frequency cutoff below 20 Hz) is a strong indication of the ability of the theoretical model to accurately predict the noise field with correct relative levels recorded by the three different sensors. The effect of propagation is quite clear when comparing Figs. 5, 7, and 8. Below 20 Hz, the data show a rise in level below 20 Hz of 40–50 dB. Figure 5 indicates that much of this increase in level is a propagation effect so that, in Fig. 8, the increase in source level is only 20–30 dB. Hence, we have the strong indication that it is necessary to account for propagation effects when extracting noise source levels from measured noise data.

For completeness in demonstrating this procedure for determining the noise source level, Fig. 9 shows the noise source levels derived from data taken for different sea states. As expected, the noise source level increases with increasing sea state in the region below 60–70 Hz, possibly indicating man-made noise dominating in the adjacent higher frequency regime.[21]

III. COMPARISON WITH OTHER SHALLOW WATER SEISMIC NOISE RESULTS

Kibblewhite and Ewans[1] have reported extensively on a series of experiments to measure seismic noise; their goal was to investigate the origin of this noise. Geophones were placed at the shore close to a relatively flat area of the continental shelf, with an average water depth of 100 m. In Ref. 1 the geophone data were converted to source strength at the sea surface based on the assumption that the seismic field at the receiver was representative of the seismic field on the seabed. The measured particle displacements were translated into source levels by means of a simple impedance relation assuming the bottom to be a fluid half-space.[1]

The above analysis for the very similar Ligurian shelf environment suggests that these two assumptions are in fact inconsistent. A fluid bottom provides no mechanism for the very low-frequency sound in a significant amount to propagate from the sources at sea to the receiver on land. Propagation modeling based on the fluid environmental model would therefore indicate significant differences in the particle displacements on the seabed and on land. If, however, the bottom is treated as a realistic stratified elastic medium, the shear waves provide a significant propagation mechanism at the low frequencies considered, which justifies the first assumption concerning the extrapolation of the shore data to seabed displacements.

Adopting this assumption, we will here repeat the procedure described above to analyze the propagation effects embedded in the New Zealand data and subsequently derive the source spectrum. The results indicate that correcting for environmental propagation conditions yields consistent noise source levels independent of the location from which the data were obtained.

The limitations of the simple fluid bottom impedance approach were acknowledged in Ref. 1, and Kibblewhite has

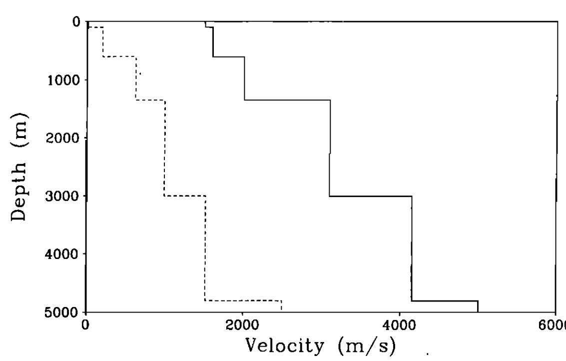

FIG. 10. Geophysical model for the New Zealand continental shelf used for modeling the propagation effect imbedded in the low-frequency ambient noise data obtained by Kibblewhite and Evans.[1] The water depth is 100 m and the bottom is represented by a series of elastic layers overlying a homogeneous subbottom starting at a depth of 4800 m. The compressional and shear speeds are indicated by the solid and dashed curves, respectively.[23]

later performed a more-detailed analysis of the effect of shear on the noise propagation.[22] In contrast to the present full stratification treatment, however, the analysis was done on an interface by interface basis, believed to underestimate the shear wave effect.

The geophysical model for the area of the New Zealand experiments[1] is shown in Fig. 10.[23] The bottom is represented by a series of elastic layers overlying a homogeneous subbottom starting at a depth of 4800 m.

As discussed in Sec. I, an analysis of the Green's function $g(k;z,z')$ provides insight into the spectral partitioning of noise. Rather than plotting the Green's functions for each frequency, they can conveniently be "stacked" and contoured. For this purpose, rather than using the horizontal wavenumber as the abcissa of the contour plot, it is convenient to use the frequency-independent horizontal slowness $s = 1/c = k/\omega$, with c the horizontal phase velocity. Figure 11 shows the contours of the horizontal and vertical component Green's functions. Note that horizontal slices yield the type of plots shown in Fig. 3 and hence the contribution to the noise level at any frequency is obtained by integrating along a horizontal slice. The structure of the Green's functions can be related to representative velocities of the seismic structure. Thus, for example, at higher frequencies we see a slowness cutoff of about 5.6 s/km for the "fundamental mode" corresponding to the Sholte wave's asymptotic velocity of about 0.9 times the shear speed in the uppermost sedimentary layer: 0.9×200 m/s $\approx 1/5.6$ s/km. The other seis-

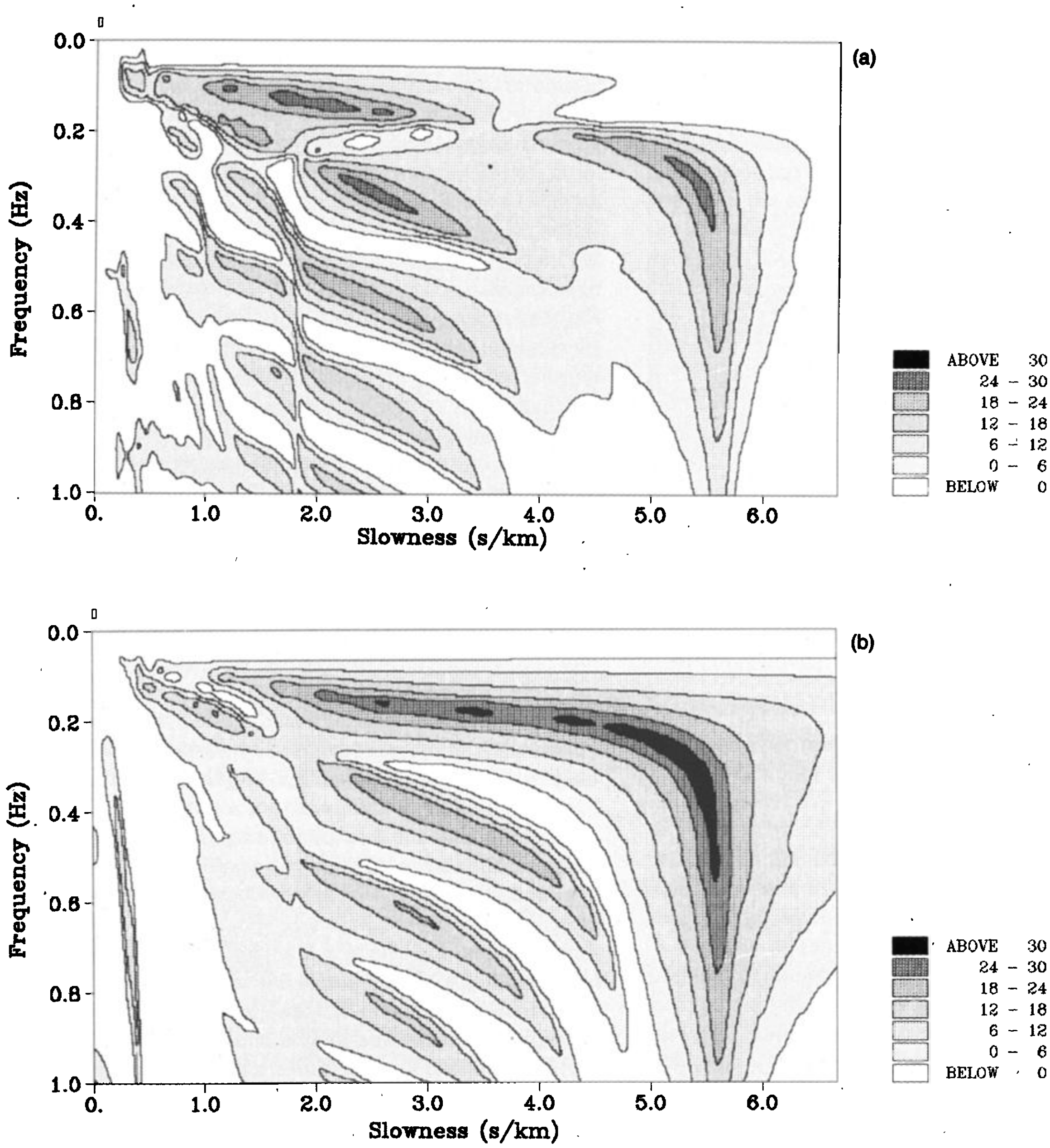

FIG. 11. Contours of the kernels of Eq. (5) for: (a) horizontal particle velocity and (b) vertical particle velocity as a function of frequency and horizontal slowness. The evanescent spectrum in the water column covers slownesses in excess of 0.67 s/km, and the dominance of this part of the propagation spectrum is evident.

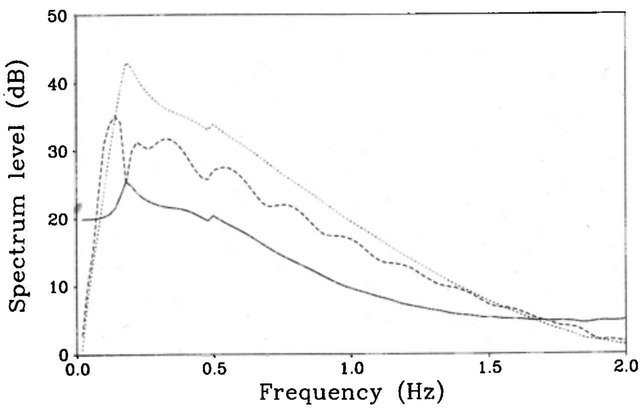

FIG. 12. Simulated noise spectra for New Zealand environment at frequencies below 2 Hz for hydrophone (solid line), horizontal geophone (dashed line), and vertical geophone (dotted line). The source level is 0 dB at all frequencies and the magnification due to the seismic propagation is evident, with up to 25-dB gain for the hydrophone component. When compared to the high-frequency level above 2 Hz, the magnification of the geophone components is even larger, with up to 50-dB magnification on the vertical geophone at 0.2 Hz.

mic "modes" or branches of these contour plots have transition regions associated with the shear speeds of the deeper layers.

The *continuous* and *discrete* parts of the spectrum correspond to slownesses of less than 0.67 s/km [1/(1500 m/s)] so that Fig. 11 clearly indicates virtually no contribution from this plane-wave portion of the spectrum below 1 Hz. Only this part of the spectrum will contribute to the field if the bottom is fluid. The *evanescent* spectrum in the water column corresponds to slowness of greater than 0.67 s/km and obviously is the dominant contribution to the noise. This clearly shows that a simplistic interpretation of the distribution of seismic noise in terms of plane-wave concepts for fluid media is misleading at low frequencies.

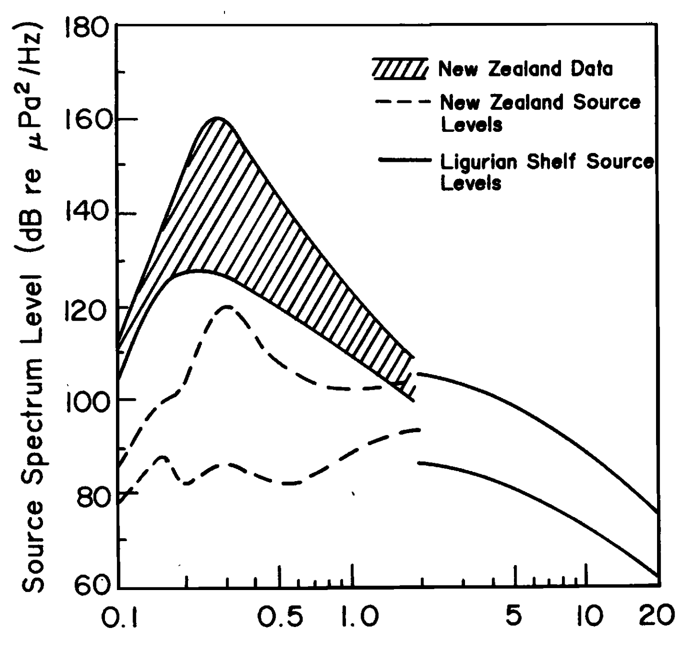

FIG. 13. Comparison of low to high sea state source level envelopes obtained from Ligurian shelf data (solid lines) and New Zealand data (dashed line) with ambient noise data presented by Kibblewhite and Evans,[1] as indicated by the hatched area. The consistency of the source levels obtained in the two different geographical areas is evident.

Figure 12 shows simulated noise spectra for the New Zealand environment for a source level of 0 dB at all frequencies and therefore directly displays the propagation "magnification" for the hydrophone. The magnification due to the guided seismic propagation is as much as 25 dB for the hydrophone component. When compared to the levels above 2 Hz, the "magnification" of the geophone components is even larger—up to 50 dB, for the vertical geophone at 0.2 Hz. Figure 13 indicates Kibblewhite's and Ewans[1] derived source level results as the hatched area. The dashed lines indicate the low to high sea state source spectrum envelope obtained by converting these "source levels" to particle velocity by the impedance relation used by Kibblewhite and Ewans, followed by subtraction of the vertical particle velocity spectrum of Fig. 12.[1]

In Fig. 13, we have included the higher frequency source levels derived in Sec. II for the Ligurian shelf data, as indicated by the solid lines. The consistency of the extracted source levels for the two different geographical areas and adjacent frequency regimes is evident. It is interesting to note that the "noise floor" at low sea states has been leveled

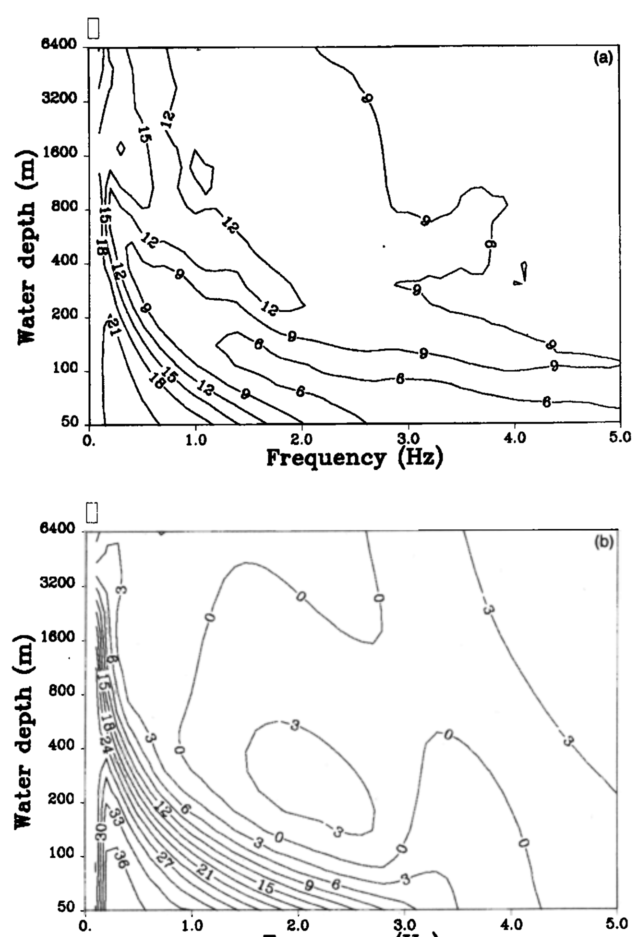

FIG. 14. Propagation "magnification" of ambient noise as a function of water depth and frequency, illustrated in the form of contours of the levels obtained for source level Q^2 corresponding to 0 dB on: (a) a hydrophone and (b) a vertical geophone on the seabed, in water depths ranging from 50 to 6400 m. The bottom is represented by the environmental model shown in Fig. 10.

out significantly compared to the measured data. The same is the case for the high sea state source levels, except for a narrow band around 0.3 Hz, where a 20-dB rise in source level appears. This behavior suggests that at low sea states the noise is dominated by a single source mechanism with a relatively flat frequency spectrum, whereas a second, more narrow-banded mechanism becomes important at higher sea states.

It should be pointed out that the small ± 5 dB variations in the derived source levels are probably due to smoothing of the hatched area envelope and mismatches in the environmental model. They should therefore at this point not be associated with any physical phenomenon.

IV. EFFECT OF WATER DEPTH ON NOISE LEVEL

Kibblewhite and Ewans[1] compared the New Zealand data with other seismic experiments in an assortment of locations and water depths. However, as shown above, a comparison of associated source levels requires that the propagation effects be removed. Since geophysical models were not readily available for the other data sets, a quantitative analysis of these data, similar to the ones described above, has not been performed.

A qualitative estimate of the propagation "magnification" imbedded in these data sets can be obtained, however, by investigating the effect of the water depth alone. The result of such a study is shown in Fig. 14(a) in the form of contours of the "magnification" of the hydrophone levels due to propagation effects as a function of frequency and water depth. The New Zealand geophysical model (Fig. 10) was assumed to be representative and was therefore used for all water depths. Although the "magnification" is not easily defined for the geophone components, Fig. 14(b) indicates the associated levels predicted for a vertical geophone on the bottom and clearly demonstrates the even higher propagation effect on this component, with a difference in spectral level of 40 dB between the low-frequency/shallow water and the high-frequency/deep water values as opposed to approximately 20 dB for the hydrophone levels of Fig. 14(a).

Although a generic environmental model was used for calculating the "magnification" as a function of water depth in Fig. 14(a), at least a rough estimate of source levels in other areas can be obtained by subtraction of the predicted values from available data sets. In fact, when doing this for the deep water data presented for comparison purposes by Kibblewhite and Ewans,[1] the derived source levels all overlap with the source levels obtained from the New Zealand and Ligurian shelf data in Fig. 13, significantly reducing the spread observed in the original data.

V. CONCLUSION

A previously developed theory for surface-generated noise in a stratified medium has been combined with a full wave solution technique yielding exact field representations for a stratified seismoacoustic environment. The resulting numerical model has been applied to investigate the basic propagation features of low-frequency surface-generated ambient noise.

It has been demonstrated that the propagation effects manifest themselves in an effective "magnification" resulting from guided wave effects, clearly indicating the importance of including propagation effects when determining seismic noise source levels from data obtained from hydrophones and geophones.

The model has been used to analyze data from two shallow water, seismoacoustic experiments in different geographical areas and adjacent frequency regimes, with consistent estimates of source levels as a result.

The significant variation of the propagation "magnification" as a function of water depth has been demonstrated. When removing the propagation effects from different deep water data presented in the literature, the derived source levels turn out to be consistent with those obtained in shallow water, in contrast to the original data.

Across the frequency band of 0.1–10 Hz the consistency in derived source level for both shallow and deep water data suggests that a single source mechanism may account for most of the seismoacoustic noise at low sea states, whereas a second mechanism appears about 0.25 Hz above some threshold sea state (Fig. 13). This particular sea state dependence of the spectral level of the noise becomes apparent only after we account for propagation mechanisms. In fact, Fig. 13 is a perfect example of how the double-logarithmic representation over a large dynamic range may lead to false conclusions: The low sea state envelope appears as having the same qualitative behavior as the high sea state envelope, where, in fact, the frequency dependence at low sea state is essentially all accounted for by the propagation.

In general, the results make it clear that *measured* noise level should not be mistaken for noise *source* level.

ACKNOWLEDGMENTS

The work was supported in part by the Office of Naval Research, Arctic Program Office. The authors would like to thank Tuncay Akal, SACLANT ASW Research Centre, Italy and Alec Kibblewhite, University of Auckland, New Zealand for their willingness to supply experimental and environmental data for this study.

[1]A. C. Kibblewhite and K. C. Ewans, "Wave–wave interactions, microseisms, and infrasonic ambient noise in the ocean," J. Acoust. Soc. Am. **78**, 981–994 (1985).

[2]W. A. Kuperman and F. Ingenito, "Spatial correlation of surface generated noise in a stratified ocean," J. Acoust. Soc. Am. **67**, 1988–1996 (1980).

[3]R. Hamson, "The theoretical responses of vertical and horizontal line arrays on wind-induced noise in shallow water," J. Acoust. Soc. Am. **78**, 1702–1712 (1985).

[4]W. A. Kuperman and M. C. Ferla, "A shallow water experiment to determine the source spectrum level of wind-generated noise," J. Acoust. Soc. Am. **77**, 2067–2073 (1985).

[5]F. Ingenito and S. N. Wolf, "Site dependence of wind-dominated ambient noise in shallow water," J. Acoust. Soc. Am. **89** (1989) (to be published).

[6]H. Schmidt, "Excitation and propagation of interface waves in a stratified seabed," in *Acoustics and the Sea-bed*, edited by P. C. Pace (Bath U. P., Bath, England, 1983).

[7]T. Akal, A. Barbagelata, G. Guido, and M. Snoek, "Time dependence of ambient seafloor noise on a continental shelf," in *Ocean Seismo-Acoustics*, edited by T. Akal and J. M. Berkson (Plenum, New York, 1986).

[8]A. J. Perrone, "Infrasonic and low-frequency ambient noise measurements on the Grand Banks," J. Acoust. Soc. Am. **55**, 754–758 (1974).

[9]R. H. Nichols, "Infrasonic ambient ocean noise measurements: Eleuthera," J. Acoust. Soc. Am. 69, 974–981 (1981).

[10]T. E. Talpey and R. D. Worley, "Infrasonic ambient noise measurements in deep Atlantic water," J. Acoust. Soc. Am. 75, 621–622 (1984).

[11]K. Hasselman, "A statistical analysis of the generation of microseisms," Rev. Geophys. 1, 177–210 (1963).

[12]R. G. Adair, J. A. Orcott, and T. H. Jordan, "Low-frequency noise observations in the deep ocean," J. Acoust. Soc. Am. 80, 633–645 (1986).

[13]B. Kerman, *Sea Surface Sound* (Kluwer, Dordrecht, The Netherlands, 1988).

[14]H. Schmidt and J. Glattetre, "A fast field model for three-dimensional wave propagation in stratified environments based on the global matrix method," J. Acoust. Soc. Am. 78, 2105–2114 (1985).

[15]H. Schmidt and F. B. Jensen, "A full wave solution for propagation in multilayered viscoelastic media with application to Gaussian beam reflection at fluid–solid interfaces," J. Acoust. Soc. Am. 77, 813–825 (1985).

[16]H. Schmidt and G. Tango, "Efficient global matrix approach to the computation of synthetic seismograms," Geophys. J. R. Astron. Soc. 84, 331–359 (1986).

[17]H. Schmidt, *SAFARI: Seismo-Acoustic Fast Field Algorithm for Range Independent Environments. User's Guide* (SACLANT ASW Research Centre, La Spezia, Italy, 1987), SR 113.

[18]F. B. Jensen and W. A. Kuperman, "Optimum frequency of propagation in shallow water environments," J. Acoust. Soc. Am. 73, 813–819 (1983).

[19]D. Rauch, "On the role of bottom interface waves in ocean seismoacoustics: a review," in *Ocean Seismo-Acoustics*, edited by T. Akal and J. M. Berkson (Plenum, New York, 1986).

[20]F. B. Jensen and H. Schmidt, "Shear properties of ocean sediments determined from numerical modelling of Scholte wave data," in *Ocean Seismo-Acoustics*, edited by T. Akal and J. M. Berkson (Plenum, New York, 1986).

[21]W. A. Kuperman, "Propagation effects associated with ambient noise," in *Sea Surface Sound*, edited by B. Kerman (Kluwer, Dordrecht, The Netherlands, 1988).

[22]A. C. Kibblewhite, "Ocean noise spectrum below 10 Hz—mechanisms and measurements," in *Sea Surface Sound*, edited by B. Kerman (Kluwer, Dordrecht, The Netherlands, 1988).

[23]A. C. Kibblewhite (private communication, 1987).